

Tet2 promotes pathogen infection-induced myelopoiesis through mRNA oxidation

Qicong Shen^{1*}, Qian Zhang^{1,2*}, Yang Shi³, Qingzhu Shi³, Yanyan Jiang¹, Yan Gu¹, Zhiqing Li³, Xia Li², Kai Zhao², Chunmei Wang², Nan Li¹ & Xuetao Cao^{1,2}

Varieties of RNA modification form the epitranscriptome for post-transcriptional regulation¹. 5-Methylcytosine (5-mC) is a sparse RNA modification in messenger RNA (mRNA) under physiological conditions². The function of RNA 5-hydroxymethylcytosine (5-hmC) oxidized by ten-eleven translocation (Tet) proteins in *Drosophila* has been revealed more recently^{3,4}. However, the turnover and function of 5-mC in mammalian mRNA have been largely unknown. Tet2 suppresses myeloid malignancies mostly in an enzymatic activity-dependent manner⁵, and is important in resolving inflammatory response in an enzymatic activity-independent way⁶. Myelopoiesis is a common host immune response in acute and chronic infections; however, its epigenetic mechanism needs to be identified. Here we demonstrate that Tet2 promotes infection-induced myelopoiesis in an mRNA oxidation-dependent manner through Adar1-mediated repression of Socs3 expression at the post-transcriptional level. Tet2 promotes both abdominal sepsis-induced emergency myelopoiesis and parasite-induced mast cell expansion through decreasing mRNA levels of Socs3, a key negative regulator of the JAK–STAT pathway that is critical for cytokine-induced myelopoiesis. Tet2 represses Socs3 expression through Adar1, which binds and destabilizes Socs3 mRNA in a RNA editing-independent manner. For the underlying mechanism of Tet2 regulation at the mRNA level, Tet2 mediates oxidation of 5-mC in mRNA. Tet2 deficiency leads to the transcriptome-wide appearance of methylated cytosines, including ones in the 3' untranslated region of Socs3, which influences double-stranded RNA formation for Adar1 binding, probably through cytosine methylation-specific readers, such as RNA helicases. Our study reveals a previously unknown regulatory role of Tet2 at the epitranscriptomic level, promoting myelopoiesis during infection in the mammalian system by decreasing 5-mCs in mRNAs. Moreover, the inhibitory function of cytosine methylation on double-stranded RNA formation and Adar1 binding in mRNA reveals its new physiological role in the mammalian system.

During infection, sensing pathogen and inflammatory cytokines skews haematopoiesis towards myeloid development; however, the epigenetic mechanism for this pathogen infection-induced myelopoiesis is unclear⁷. We investigated the role of Tet2, a myeloid tumour suppressor, in pathogen infection-induced myelopoiesis. First, we subjected Tet2-deficient (knockout) and the littermate control (wild-type) mice to caecal ligation and puncture (CLP), a model of abdominal polymicrobial sepsis with acute mobilization and expansion of myeloid cells. Compared with the control mice, Tet2-deficient mice were protected from sepsis with lower mortality rates (Fig. 1a, see graph Source Data for statistics) and had lower clinical scores (Fig. 1b). The bactericidal activity of Tet2-deficient mice was not significantly affected within 24 h (Fig. 1c). One day after CLP, only the control mice developed obvious neutrophilia and inflammatory monocytosis,

whereas the neutrophil and monocyte numbers barely varied in Tet2-deficient mice (Fig. 1d). Significantly fewer peritoneal neutrophils and monocytes were also observed in Tet2-deficient mice (Fig. 1e). The increased neutrophil and monocyte numbers in control mice were associated with higher serum levels of inflammatory cytokines, such as tumour necrosis factor, keratinocyte chemoattractant and macrophage inflammatory protein-1 α , compared with Tet2-deficient mice (Fig. 1f). In a mouse model infected with parasite *Schistosoma japonicum* (Extended Data Fig. 1a), the numbers of mast cells in *Kit*^{W-sh/W-sh} mice transplanted with Tet2-deficient bone marrow cells were lower than those in the control group in the jejunum and ileum with diffuse mucosal inflammation and granulomatous reaction (Extended Data Fig. 1b, c). These data show that Tet2 promoted both emergency myelopoiesis, fuelling a cytokine storm during abdominal sepsis, and a long process of myelopoiesis, promoting expansion of tissue mast cells derived from bone marrow progenitor cells during chronic parasite infection.

We subjected significant varied genes in RNA sequencing (RNA-seq) data (Supplementary Table 1) from Tet2-deficient bone-marrow-derived mast cells (BMMCs) and control cells to Kyoto Encyclopedia of Genes and Genomes (KEGG) pathway analysis; and the expression variations of the genes in JAK–STAT and PI3K–AKT pathways, which are critical for inflammatory cytokine-induced myelopoiesis^{8,9}, were labelled near scatter plots (Fig. 2a). Among these genes, *Socs3*, a key suppressor of JAK–STAT signalling, was significantly increased in the Tet2-deficient group. Upregulation of *Socs3* in both BMMCs and Lin[−]Kit⁺ haematopoietic stem and progenitor cells (HSPCs) stimulated by interleukin-3 (IL-3), a critical cytokine for both acute infection-induced myelopoiesis⁸ and parasite infection-induced mast cell expansion⁹, was observed at both mRNA and protein levels in Tet2-deficient groups (Fig. 2b–d; see Supplementary Fig. 1 for gel Source Data). We also found decreased expression of IL-3 signal-induced genes in Tet2-deficient BMMCs (Extended Data Fig. 2a–c) and the impaired phosphorylation of Akt and STAT5 in both IL-3-stimulated BMMCs and bone marrow cells from Tet2-deficient mice (Extended Data Fig. 2d, e), further validating the defective JAK–STAT signalling in Tet2-deficient myeloid cells. Silencing of *Socs3* in Tet2-deficient BMMCs increased IL-3 signalling (Extended Data Fig. 2f), indicating that Tet2 promoted infection-induced myelopoiesis by repressing *Socs3* expression for efficient cytokine signalling.

To reveal the molecular mechanism of Tet2-mediated *Socs3* suppression, we first detected the DNA methylation levels of CpGs in two predicted CpG islands near the *Socs3* promoter, and found that all of these CpGs were hypomethylated in both wild-type and Tet2-deficient BMMCs (Extended Data Fig. 3a, b); loss of Tet2 still increased the mRNA level of *Socs3* when *de novo* transcription was inhibited (Extended Data Fig. 3c), indicating the potential role of Tet2 in regulating *Socs3* at post-transcriptional level.

¹National Key Laboratory of Medical Immunology & Institute of Immunology, Second Military Medical University, Shanghai 200433, China. ²Department of Immunology & Center for Immunotherapy, Institute of Basic Medical Sciences, Peking Union Medical College, Chinese Academy of Medical Sciences, Beijing 100005, China. ³Institute of Immunology, Zhejiang University School of Medicine, Hangzhou 310058, China.

*These authors contributed equally to this work.

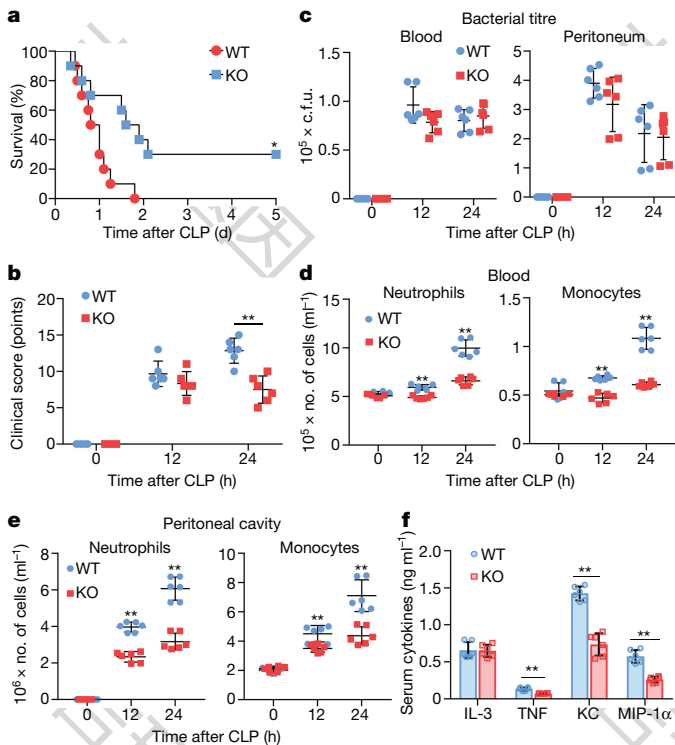


Figure 1 | Reduced emergency myelopoiesis in Tet2-deficient mice in abdominal sepsis. a–f, Comparison of Tet2-deficient (KO) and the littermate control (WT) mice in the CLP model. a, Kaplan–Meier survival curve ($n = 10$). b, c, Clinical scores and bacterial titre ($n = 6$) (c.f.u., colony-forming units). d, e, Cell enumeration ($n = 6$). f, Levels of cytokines in serum 1 day after CLP ($n = 6$ biologically independent mice). TNF, tumour necrosis factor; KC, keratinocyte chemoattractant; MIP-1 α , macrophage inflammatory protein-1 α . * $P < 0.05$, ** $P < 0.01$ (Kaplan–Meier (a) or unpaired two-sided Student’s t -test, mean and s.d. (b–f)). n , number of biologically independent animals.

Tet2 was recently identified as an RNA-binding protein, implying its general role in post-transcriptional regulation¹⁰. We performed three biological replicates of enhanced crosslinking and immunoprecipitation followed by high-throughput sequencing (eCLIP-seq)¹¹ for obtaining potential Tet2-binding RNAs in BMMCs (Extended Data Fig. 3d, e), and biological replicates correlated well with each other (Extended Data Fig. 3f). Among thousands of peaks identified in the three replicates, more than 80% were located in genic regions (Fig. 2e), including *Socs3* loci (Supplementary Table 2), and about 50–60% of CLIP peaks overlapped with each other in at least two replicates (Fig. 2f).

In RNA-seq data, we found more A-to-G mutations transcriptome-wide in the wild-type group than in the Tet2-deficient group, which contained an A-to-G mutation in the 3′ UTR of *Socs3* (Supplementary Table 3). Most of the group-specific A-to-G mutants showed low mutation rates (Fig. 2g), and were more distributed in 3′ UTRs in mature mRNA elements (Fig. 2h), consistent with RNA editing preferences in mRNAs. Furthermore, top motifs across the mutation sites identified by homer software¹² were found in the published motif across RNA A-to-I editing sites by adenosine deaminase Adar1 (ref. 13), implying a contribution of Adar1 to these mutations. Furthermore, the top motif in Tet2 CLIP peaks was also similar to the last seven bases of the published motif (Fig. 2i), implying a regulatory role of Tet2 in RNA editing.

Adar1 binds double-stranded RNA (dsRNA) and edits nearby adenosines¹³. Prediction of the secondary structure of the 3′ UTR of *Socs3* showed that the A-to-G mutant was in a dsRNA stem loop (Extended Data Fig. 4a). The 3′ UTR of *Lrrc47* bearing an A-to-G mutant in a predicted dsRNA stem in wild-type BMMCs was used as a classic control (Extended Data Fig. 4b). We validated that the

A-to-G mutation appeared in the 3′ UTR of *Socs3* in wild-type BMMCs (Extended Data Fig. 4c). Adar1 binding in the 3′ UTR of *Socs3* and *Lrrc47* in wild-type BMMCs was also validated (Fig. 3a and Extended Data Fig. 4d, e). Editing levels in the 3′ UTR of *Socs3* gradually increased during differentiation of BMMCs (Extended Data Fig. 4f). Tet2 loss barely changed protein levels of Adar1, which located mainly in the nuclei of BMMCs (Extended Data Fig. 4g, h). Silencing of Adar1 indeed decreased editing rates of the sites in the 3′ UTR of *Socs3* and *Lrrc47* (Fig. 3b and Extended Data Fig. 4i).

Silencing Adar1 increased mRNA and protein levels of *Socs3* in wild-type BMMCs (Fig. 3c, d). Equal signals were observed for the reporters bearing the A-to-G mutated and wild-type 3′ UTR of *Socs3* (Fig. 3e). Furthermore, both wild-type Adar1 and an enzymatic activity mutant (Adar1_{E861A}), but not a dsRNA binding domain mutant (lacking N456–G743, Adar1 Δ dsRNA), repressed the signals of the reporter bearing the A-to-G mutated 3′ UTR of *Socs3* (Fig. 3f). Previous studies indicated that Adar1 also mediates post-transcriptional regulation independent of RNA editing through other RNA-binding proteins^{14,15}. Through immunoprecipitation-coupled liquid chromatography–tandem mass spectrometry (LC–MS/MS) analysis as previously reported⁶, we found that Adar1 associated with two RNA-binding proteins (Fig. 3g), which were involved in regulating mRNA processing and stability^{16,17}. This implies that Adar1 post-transcriptionally represses *Socs3*, probably through its binding partner, which needs further investigation.

To investigate the regulatory role of Tet2 in Adar1-mediated inhibition of *Socs3* expression, we first found that silencing Adar1 in Tet2-deficient BMMCs barely increased the mRNA level of *Socs3* any further (Fig. 3h). Adar1 could inhibit both mRNA and protein levels of overexpressed *Socs3*, especially with the help of both wild-type Tet2 and a DNA-interacting residue mutant Tet2 (Tet2 Δ DNA)¹⁸, but not with an α -ketoglutarate (KG)-interacting mutant and the Fe²⁺ binding mutant of Tet2 (Tet2_{HxD}) (Fig. 3i and Extended Data Fig. 4j, k). Overexpression of Tet2 and Tet2 Δ DNA, but not Tet2_{HxD}, decreased the *Socs3* mRNAs in Tet2-deficient BMMCs (Fig. 3j). Although all three forms of Tet2 could bind *Socs3* mRNAs, a lower signal was observed in the Tet2_{HxD} mutant group (Fig. 3k), indicating that the stable catalytic structure also improves the interaction between Tet2 and *Socs3* mRNA. These results indicate that Tet2 promotes Adar1-mediated repression of *Socs3* mRNA in an enzymatic activity-dependent manner, but not in a DNA interaction-dependent manner.

Recently, 5-mC and its oxidation derivative, 5-hydroxymethylcytosine (5-hmC), catalysed by Tet proteins¹⁹, have been found in RNA in *Drosophila*³ and human cell lines⁴. We found that recombinant Tet2 could decrease 5-mC levels of transcribed RNAs *in vitro* in a substrate-dependent manner (Fig. 4a and Extended Data Fig. 5a, b). However, the major oxidation form of 5-mC *in vitro* in RNA was 5-hmC (Fig. 4b), unlike the oxidation forms in DNA (Extended Data Fig. 5c). Overexpression of wild-type Tet2 and Tet2 Δ DNA, but not Tet2_{HxD}, in HEK293T cells decreased 5-mC levels of mRNAs (Extended Data Fig. 5d–f). However, both overexpressing Tet2 in HEK293T cells and Tet2 knockout in BMMCs barely affected both the overall 5-mC levels of total RNAs and the levels of reported 5-mCs in tRNA^{Asp(GUC)} (ref. 20) (Extended Data Fig. 5g, h). Furthermore, silencing Tet2 in HEK293T cells and Tet2 knockout in BMMCs both increased 5-mC levels in mRNAs compared with the control cells (Fig. 4c and Extended Data Fig. 5i, j). However, both dot blot (800 ng mRNA) and LC–MS analysis (sensitivity 0.1 nM) barely detected signals of 5-hmC, 5-formylcytosine, (5-fC) and 5-carboxylcytosine (5-caC) in mRNAs in the tested cells (data not shown), indicating much lower levels of these oxidation products than 5-mC *in vivo*. These results indicate that Tet2 could decrease overall levels of 5-mCs in mRNAs in an oxidation-dependent manner.

To reveal 5-mC regulation by Tet2 transcriptome-wide, we performed bisulfite sequencing of mRNAs from Tet2-deficient BMMCs and the control cells. Both technical and biological replicates had good overlapping rates of identified 5-mCs, especially in Tet2-deficient group

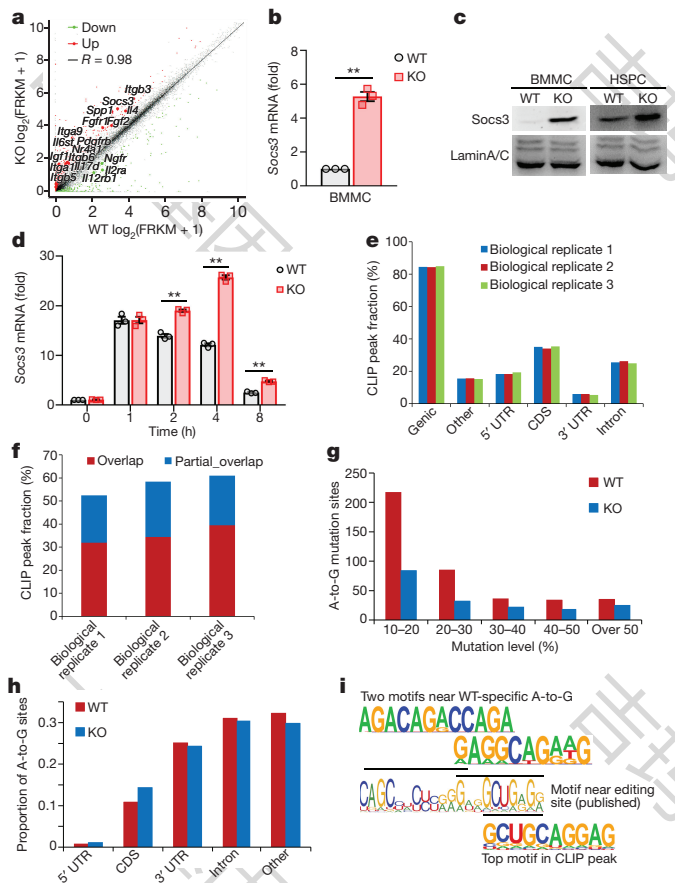


Figure 2 | Deficiency of Tet2 leads to increased transcripts and decreased A-to-I RNA editing for *Socs3*. **a**, Scatter plot of mRNA levels for a pair of Tet2-deficient (KO) and the control (WT) BMMCs. Upregulated (red) and downregulated (green) genes are coloured, varied genes in JAK–STAT and PI3K–AKT pathways are labelled near bigger plots. FRKM, fragments per kilobase of exon per million fragments mapped. **b–d**, qPCR and immunoblot assays of *Socs3* in BMMCs (**b**, **c**) and IL-3-stimulated Lin^{Kit} HSPCs for 8 h (**c**, **d**). **e**, **f**, Genomic distribution of CLIP peaks and their overlapping rates among the three biological replicates. **g**, **h**, Mutation levels and intragenic distribution of A-to-G mutants. CDS, coding sequence. **i**, Top motifs in 200 bp across A-to-G sites (top) and CLIP peaks (bottom), and the published motif (middle). * $P < 0.05$, ** $P < 0.01$, unpaired two-sided Student's *t*-test. Mean and s.e.m. of triplicate biological (**b**, **d**) replicates. Blots are representative of three independent experiments (**c**).

(Extended Data Fig. 6a, b). More methylcytosines were consistently identified, and with higher methylation levels in Tet2-deficient replicates than in controls (Fig. 4d and Extended Data Fig. 6c). There were many more group-specific methylcytosines in Tet2-deficient cells than in controls, more than half of which were located in the genic region, mostly in introns (Fig. 4e and Supplementary Table 4). As cell-specific alternative splicing leads to cell-specific intron retention, Tet2 may regulate 5-mC turnover in a cell-specific manner. Expression of genes bearing specific methylcytosines in the Tet2-deficient group or Tet2 CLIP peaks was more upregulated in Tet2-deficient cells (Extended Data Fig. 6d), implying an important role for Tet2-mediated mRNA oxidation in decreasing mRNA levels of genes such as *Socs3*. In mature mRNA-related elements, more methylcytosines located in the 3' UTR in the Tet2-deficient group than in controls (Fig. 4f), further confirming the regulatory role of Tet2 in the 3' UTR of mRNAs. When connecting the CLIP-seq data to specific methylcytosines in the Tet2-deficient group, we found that over 60% of genes or 3' UTRs bearing these methylcytosines were associated with CLIP peaks (Fig. 4g). Methylcytosines and CLIP peaks in exons located close to

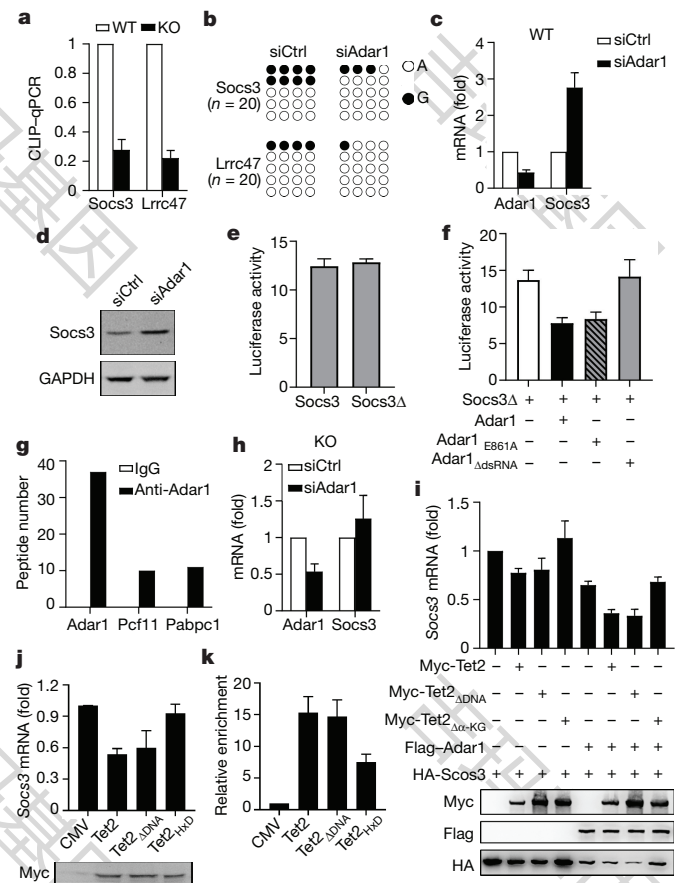


Figure 3 | Adar1 binds unmethylated *Socs3* mRNA and inhibits *Socs3* expression in a Tet2-dependent manner. **a**, qPCR analysis of editing regions in CLIPED RNAs for Adar1. **b–d**, RT-PCR-seq, qPCR and immunoblot assay of editing rates or gene expression in Adar1-silenced Tet2-knockout or wild-type BMMCs and the controls. **e**, **f**, Luciferase reporter assays of lysates of HEK293T cells transfected with pMIR plasmid with wild-type (*Socs3*) or mutant (*Socs3* Δ), and indicated plasmids for 24 h. **g**, Peptide numbers of potential Adar1 partners. **i**, qPCR and immunoblot analysis of HEK293T cells transfected for 24 h with indicated plasmids. **j**, **k**, Knockout BMMCs were transiently transfected with plasmids expressing the indicated forms of Tet2. *Socs3* mRNA levels were examined, and *Socs3* 3' UTR was from Tet2-immunoprecipitated RNA. Mean and s.d. of triplicate technical replicates (**a**, **c**, **e**, **f**, **h–k**). Blots are representative of three independent experiments (**d**, **i**, **j**).

each other in a mature mRNA view (Extended Data Fig. 6e). Among the 3' UTRs bearing several methylcytosines, *Socs3* was indeed in the list, and we validated that these methylcytosines appeared in Tet2-deficient cells (Extended Data Fig. 6f). We also found two other genes: *Zfp65* with an A-to-G mutant near methylcytosines in the 3' UTR where it was enriched in repeat elements; and *Tmed10* with a predicted stable dsRNA structure in the 3' UTR (Extended Data Fig. 6g–i). Adar1 also bound *Tmed10*, partly depending on Tet2 (Fig. 4h). We further validated increased RNA methylation levels in 3' UTRs of the three genes in Tet2-deficient BMMCs (Extended Data Fig. 6j).

We further investigated the underlying mechanism for the repressive role of 5-mC in Adar1 function, and found that overexpressed wild-type Tet2 and the Tet2 Δ DNA indeed decreased 5-mC levels of overexpressed *Socs3* mRNAs (Extended Data Fig. 7a). Oxidation forms of 5-mC in *Socs3* 3' UTR were not detected in wild-type BMMCs (Extended Data Fig. 7b). Mutating the 5-mCs in the 3' UTR of *Socs3* mRNA decreased the mRNA levels of *Socs3*, and overexpression of Tet2 barely synergistically repressed the mRNA levels of mutated *Socs3* with Adar1, compared with the wild-type *Socs3* (Extended Data Fig. 7c).

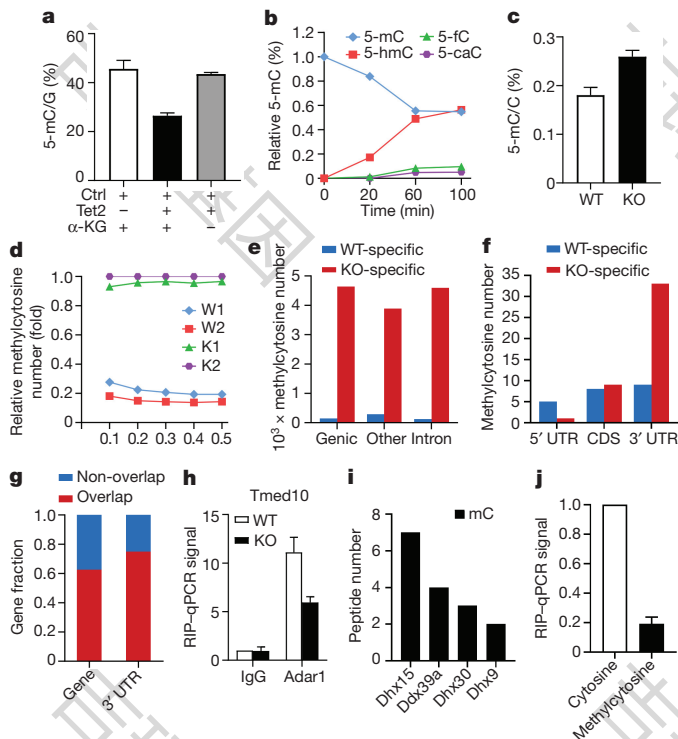


Figure 4 | Tet2 decreases mRNA methylation level in an oxidation-dependent manner for Adar1 targeting. a–c, LC–MS quantifying 5-mC and its oxides in Tet2-oxidized methylated RNAs *in vitro* (a, b) or in mRNAs (c). d, Relative methylcytosine numbers in replicate samples. e, f, Group-specific methylcytosine numbers in indicated genomic elements. g, Fractions of genes or 3' UTRs bearing specific methylcytosines in knockout group associated with CLIP peaks. h, Adar1-associated endogenous *Tmed10* 3' UTR. i, Peptide numbers of methylated *Socs3* 3' UTR-binding proteins in BMMCs. j, Adar1-associated methylcytosine- or cytosine-containing *Socs3* 3' UTR *in vitro*, normalized by the 1% input after incubation. Tet2-deficient BMMCs (KO) and the control (WT) were used (c–h). Mean and s.d. of triplicate technical replicates (a, c, h, j). RIP, RNA immunoprecipitation assay.

Overexpressed Adar1 preferentially bound the mutated form of the 3' UTR (Extended Data Fig. 7d). Furthermore, 5-mCs in the 3' UTR of *Socs3* mRNA could indeed repress the editing efficiency *in vitro* (Extended Data Fig. 7e). As dsRNA structure was essential for Adar1 binding, we found that loss of Tet2 decreased the dsRNA structure in *Socs3* mRNA (Extended Data Fig. 7f). DNA and RNA modifications can recruit specific readers to mediate epigenetic regulation. With the methylated 3' UTR of *Socs3* in pull-down assay, we identified several ATP-dependent RNA helicases (Fig. 4i), which are involved in altering RNA secondary structure and unwinding of dsRNA²¹. Adar1 indeed bound fewer methylated 3' UTRs of *Socs3* than unmethylated ones (Fig. 4j). These results imply that 5-mC in mRNA inhibits Adar1 function, probably through inhibiting dsRNA formation, which is essential for Adar1 binding.

As a type of RNA modification, 5-mC has been revealed to be important in regulating stability, protein translation and processing for tRNA, rRNA and even non-coding RNA and mRNAs^{22–27}. Our current study first revealed that Tet2 decreased 5-mC levels in mRNAs in an oxidation-dependent manner, and revealed a new function of increased 5-mC in mRNA owing to Tet2 loss in inhibiting the function of Adar1, especially in *Socs3* mRNAs (Extended Data Fig. 8a, b). Furthermore, our study revealed that Tet2 loss impaired dsRNA structure, which is essential for Adar1 function. With the data on transcriptome-wide editing sites that appeared in the wild-type control group but not the Tet2-deficient group, our study provided a general relationship between Tet2 and Adar1 function.

According to our data, amounts of 5-hmC were much lower than 5-mC in mRNA from the tested mammalian cells. Thus, additional enzymatic steps by an unknown protein may convert 5-hmC back to cytosine in mRNA. Further study will be needed to reveal this unknown mechanism, probably involving the members of the AlkB family²⁵. Moreover, our study implies that Tet2-mediated mRNA oxidation may be the critical step for RNA demethylation.

As a tumour suppressor gene, mutations of *Tet2* were largely found in myeloid malignancies and some solid cancers. For haematopoiesis, loss of Tet2 leads to increased abnormal myeloid cells in ageing⁷. And our study linked Tet2 to pathogen infection-induced myelopoiesis in an immunological way, and found that Tet2 strengthens cytokine signalling in myeloid differentiation by suppressing the repressor. Furthermore, mutations with a deficiency in enzymatic activity and downregulation of Tet2 in types of disease can lead to dysregulation of 5-mC in mRNA, which may be critically involved in the pathogenesis of myeloid disorders, such as myeloid tumours. This needs further investigation.

Online Content Methods, along with any additional Extended Data display items and Source Data, are available in the online version of the paper; references unique to these sections appear only in the online paper.

Received 22 November 2016; accepted 5 December 2017.

Published online 24 January 2018.

- Fu, Y., Dominissini, D., Rechavi, G. & He, C. Gene expression regulation mediated through reversible m⁶A RNA methylation. *Nat. Rev. Genet.* **15**, 293–306 (2014).
- Zhao, B. S., Roundtree, I. A. & He, C. Post-transcriptional gene regulation by mRNA modifications. *Nat. Rev. Mol. Cell Biol.* **18**, 31–42 (2017).
- Delatte, B. *et al.* Transcriptome-wide distribution and function of RNA hydroxymethylcytosine. *Science* **351**, 282–285 (2016).
- Fu, L. *et al.* Tet-mediated formation of 5-hydroxymethylcytosine in RNA. *J. Am. Chem. Soc.* **136**, 11582–11585 (2014).
- Álvarez-Errico, D., Vento-Tormo, R., Sieweke, M. & Ballestar, E. Epigenetic control of myeloid cell differentiation, identity and function. *Nat. Rev. Immunol.* **15**, 7–17 (2015).
- Zhang, Q. *et al.* Tet2 is required to resolve inflammation by recruiting Hdac2 to specifically repress IL-6. *Nature* **525**, 389–393 (2015).
- Moran-Crusio, K. *et al.* Tet2 loss leads to increased hematopoietic stem cell self-renewal and myeloid transformation. *Cancer Cell* **20**, 11–24 (2011).
- Weber, G. F. *et al.* Interleukin-3 amplifies acute inflammation and is a potential therapeutic target in sepsis. *Science* **347**, 1260–1265 (2015).
- Lantz, C. S. *et al.* Role for interleukin-3 in mast-cell and basophil development and in immunity to parasites. *Nature* **392**, 90–93 (1998).
- He, C. *et al.* High-resolution mapping of RNA-binding regions in the nuclear proteome of embryonic stem cells. *Mol. Cell* **64**, 416–430 (2016).
- Van Nostrand, E. L. *et al.* Robust transcriptome-wide discovery of RNA-binding protein binding sites with enhanced CLIP (eCLIP). *Nat. Methods* **13**, 508–514 (2016).
- Heinz, S. *et al.* Simple combinations of lineage-determining transcription factors prime cis-regulatory elements required for macrophage and B cell identities. *Mol. Cell* **38**, 576–589 (2010).
- Nishikura, K. A-to-I editing of coding and non-coding RNAs by ADARs. *Nat. Rev. Mol. Cell Biol.* **17**, 83–96 (2016).
- Anantharaman, A. *et al.* ADAR2 regulates RNA stability by modifying access of decay-promoting RNA-binding proteins. *Nucleic Acids Res.* **45**, 4189–4201 (2017).
- Sakurai, M. *et al.* ADAR1 controls apoptosis of stressed cells by inhibiting Staufen1-mediated mRNA decay. *Nat. Struct. Mol. Biol.* **24**, 534–543 (2017).
- Grzechnik, P., Gdula, M. R. & Proudfoot, N. J. Pcf11 orchestrates transcription termination pathways in yeast. *Genes Dev.* **29**, 849–861 (2015).
- Behm-Ansmant, I., Gatfield, D., Rehwinkel, J., Hilgers, V. & Izaurralde, E. A conserved role for cytoplasmic poly(A)-binding protein 1 (PABPC1) in nonsense-mediated mRNA decay. *EMBO J.* **26**, 1591–1601 (2007).
- Hu, L. *et al.* Crystal structure of TET2–DNA complex: insight into TET-mediated 5mC oxidation. *Cell* **155**, 1545–1555 (2013).
- Kohli, R. M. & Zhang, Y. TET enzymes, TDG and the dynamics of DNA demethylation. *Nature* **502**, 472–479 (2013).
- Goll, M. G. *et al.* Methylation of tRNA^{Asp} by the DNA methyltransferase homolog Dnmt2. *Science* **311**, 395–398 (2006).
- Jarmoskaite, I. & Russell, R. RNA helicase proteins as chaperones and remodelers. *Annu. Rev. Biochem.* **83**, 697–725 (2014).
- Popis, M. C., Blanco, S. & Frye, M. Posttranscriptional methylation of transfer and ribosomal RNA in stress response pathways, cell differentiation, and cancer. *Curr. Opin. Oncol.* **28**, 65–71 (2016).
- Amort, T. *et al.* Long non-coding RNAs as targets for cytosine methylation. *RNA Biol.* **10**, 1003–1008 (2013).

24. Hussain, S. *et al.* NSun2-mediated cytosine-5 methylation of vault noncoding RNA determines its processing into regulatory small RNAs. *Cell Reports* **4**, 255–261 (2013).
25. Aas, P. A. *et al.* Human and bacterial oxidative demethylases repair alkylation damage in both RNA and DNA. *Nature* **421**, 859–863 (2003).
26. Edelheit, S., Schwartz, S., Mumbach, M. R., Wurtzel, O. & Sorek, R. Transcriptome-wide mapping of 5-methylcytidine RNA modifications in bacteria, archaea, and yeast reveals m5C within archaeal mRNAs. *PLoS Genet.* **9**, e1003602 (2013).
27. Luo, Y., Feng, J., Xu, Q., Wang, W. & Wang, X. NSun2 deficiency protects endothelium from inflammation via mRNA methylation of ICAM-1. *Circ. Res.* **118**, 944–956 (2016).

Supplementary Information is available in the online version of the paper.

Acknowledgements We thank R. L. Levine for providing Tet2 knockout mice, and K. Wang and C. Yi for helping with LC–MS analysis of RNA methylation. We thank C. Hu and W. Huang for technician support. This work was supported by grants from the National Natural Science Foundation of China (81788101, 31390431, 91542204, 31670884), the Shanghai Rising-Star Program

(17QA1405300) and the CAMS Innovation Fund for Medical Science (2016-12M-1-003).

Author Contributions X.C. designed and supervised the study. X.C., Q.Z. and Q.She. analysed the data and wrote the manuscript. Q.She. established pathogen infection mouse models. Q.She. and Q.Z. confirmed and genotyped mice, performed RNA methylation- and RNA editing-related experiments and analysed all the data of this study. Q.She. and Q.Z. performed CLIP, bisulfite sequencing and analysed the sequencing data. Y.S. performed the dot plot assays. Q.She. and Q. Shi constructed plasmids with aid from Q.Z. Y.J. performed parasite infections of mice. Y.G. and Z.L. sorted and analysed immune cells. X.L., K.Z., C.W. and N.L. provided reagents and advice.

Author Information Reprints and permissions information is available at www.nature.com/reprints. The authors declare no competing financial interests. Readers are welcome to comment on the online version of the paper. Publisher's note: Springer Nature remains neutral with regard to jurisdictional claims in published maps and institutional affiliations. Correspondence and requests for materials should be addressed to X.C. (caoxt@immunol.org).

METHODS

Mice and reagents. C57BL/6 mice were obtained from Joint Ventures Sipper BK Experimental Animal Company (Shanghai). Tet2-deficient mice on a C57BL/6 \times 129/SvEv background were provided by R. L. Levine, and backcrossed to the C57BL/6 background in our laboratory. *Kit^{W^{sh}/W^{sh}}* mice were obtained from The Jackson Laboratory. All animal experiments were undertaken in accordance with the National Institute of Health Guide for the Care and Use of Laboratory Animals, with the approval of the Scientific Investigation Board of Second Military Medical University, Shanghai. Recombinant SCF and IL-3 were from PeproTech. Antibodies used were as follows: Anti-5-mC antibody (A3001, 10G4, lot: 2RC180672, Zymo Research), Anti-5-hmC antibody (Mab-31HMC, lot: 001, Diagenode), Anti-5-fC antibody (61227, lot: 34711001, Active Motif), Anti-5-caC antibody (61225, lot: 34711001, Active Motif), Anti-Adar1 antibody (A303-884A, Bethyl Labs), Anti-Socs3 (2923, lot: 2, Cell Signaling Technology), Anti-STAT5 (9363P, lot: 3, Cell Signaling Technology), Anti-STAT5 phosphorylated (Tyr694) (9359P, C11C5, lot: 4, Cell Signaling Technology), Anti-Akt (pan) (4685, 11E7, lot: 3, Cell Signaling Technology), Anti-Akt phosphorylated (Ser473) (4060, D9E, lot: 19, Cell Signaling Technology), Anti-ERK phosphorylated (Thr202/Tyr204) (4370, D13.14.4E, lot: 6, Cell Signaling Technology), Anti-ERK (9102, lot: 23, Cell Signaling Technology), Anti-JNK phosphorylated (Thr183/Tyr185) (4668, 81E11, lot: 9, Cell Signaling Technology), Anti-JNK (9258, 56G8, lot: 11, Cell Signaling Technology), Anti-Myc (2276, 9B11, lot: 24, Cell Signaling Technology), Anti-Flag (F1804, lot: SLBJ4607V, Sigma-Aldrich), Anti-HA (3724, lot: 3, Cell Signaling Technology), Anti-LaminA/C (4777, 4C11, lot: 9, Cell Signaling Technology), Anti-GAPDH (2118, 14C10, lot: 8, Cell Signaling Technology), Anti-Tet2 (MABE462, lot: Q2141878, Millipore), Anti-J2 monoclonal antibody (10010200, IgG2a, lot: No.J21611 Scions), Anti- β -actin (3700, 8H10D10, lot: 13, Cell Signaling Technology), Anti-rabbit IgG-HRP (31460, lot: RB230194, Thermo Fisher Scientific), Anti-mouse IgG-HRP (31430, lot: RA230188, Thermo Fisher Scientific), Anti-biotin (ab6643, lot: GR99377-4, Abcam), APC anti-Kit (17-1171-81, 2B8, lot: E07202-1631, eBioscience), PerCP cyanine5.5 anti-CD11b (45-0112-82, M1/70, lot: 4301974, eBioscience), PE cyanine7 anti-Fc ϵ RI (25-5898-80, MAR-1, lot: E16926-105, eBioscience), FITC anti-Ly6G (127606, 1A8, lot: B164314, Biolegend), Alexa Fluor 700 anti-Ly6C (128024, HK1.4, lot: B224165, Biolegend), BV421 anti-F4/80 (123137, BM8, lot: B202010, Biolegend). All the antibodies are all commercially available and validated by the suppliers according to the validation statements on the manufacturers' websites.

Cell purification and cultures. For BMMCs, mouse bone marrow cells were isolated from femurs and cultured in RPMI1640 medium plus 10% (v/v) FBS (Gibco) with 10 ng ml⁻¹ IL-3 and 5 ng ml⁻¹ SCF. Half of the medium was replaced by fresh medium with cytokines every 2–3 days during culture. After 4–6 weeks in culture, BMMCs were stained to confirm the surface expression of Fc ϵ RI and Kit. Cells with purity greater than 97.5% were used for subsequent experiments. For HSPCs, bone marrow cells were stained with anti-Lineage-PE and anti-Kit-APC antibodies, and the HSPCs (purity > 99%) were sorted using a MoFloXDP High-performance Cell Sorter (DACO Cytomatix). Cells were defined as monocytes (Ly6G⁻Ly6C^{high}CD11b^{low}), neutrophils (Ly6G⁺Ly6C^{int}CD11b⁺F4/80⁻), HSPC (Kit⁺Lin⁻) and mast cells (Fc ϵ RI⁺Kit⁺). HEK293T cells were from American Type Culture Collection and cultured in endotoxin-free DMEM (Thermo Fisher Scientific) supplemented with 10% (v/v) FBS (Thermo Fisher Scientific) without further authentication and mycoplasma contamination test.

Animal models. CLP. Six-week-old mice were used in this study. The rodent model of sepsis was performed as previously described²⁸. All experiments included age-matched controls. To induce mid-grade CLP, approximately 30–50% of the caecum was ligated. To induce high-grade CLP, approximately 60–80% of the caecum was ligated. Only experiments testing survival used high-grade CLP. The clinical score of animals was assessed as previously described⁸.

Parasite infection. Female 6-week-old mast-cell-deficient (*Kit^{W^{sh}/W^{sh}}*) mice had been reconstituted with bone marrow cells from the donor mice. Then, each of the mice was infected with *S. japonicum* by skin contact with 20 cercariae, with at least 6 mice in each group. Successful infection was confirmed by the detection of parasite eggs by stool examination before use in the subsequent experiments.

RNA quantification. RNA was extracted with TRIzol reagent (Thermo Fisher Scientific) and reverse-transcribed with a reverse transcription system (Toyobo). Reverse transcription products of different samples were amplified by a LightCycler System (Roche) using the SYBR Green PCR Premix Ex Taq (Takara) according to the manufacturer's instructions, and data were normalized by the level of β -actin or 1% input RNAs in each individual sample. The 2^{- $\Delta\Delta$ C_t} method was used to calculate relative expression changes. With the help of dissociation curve analysis and the sequencing of PCR products, pairs of specific primers of each cDNA were designed and selected, without any primer dimers or unspecific amplification detected. The sequences of the primers for quantitative RT-PCR are in Extended Data Table 1.

Biochemical assay of Tet2-mediated oxidation of 5-mC in RNA. The Tet2-mediated RNA oxidation assay was conducted with the experimental workflows as previously reported²⁹, with the presence of RNasin Plus RNase Inhibitor (Promega). A reaction mixture contained 250 ng of 5-mC-bearing 3' UTR of *Socs3*, the catalytic domain of recombinant human Tet2 (active motif) or immunoprecipitated Tet2 mutants overexpressed in HEK293T cells, oxidation reagent 1 (1.5 mM Fe(NH₄)₂(SO₄)₂·6H₂O), with (α -KG+ group) or without (α -KG- group) oxidation reagent 2 (333 mM NaCl, 167 mM HEPES (pH 8.0), 4 mM ATP, 8.3 mM DTT, 3.3 mM α -KG and 6.7 mM L-ascorbic acid). The 3' UTRs of *Socs3* were obtained from *in vitro* transcription by using T7 RNA polymerase (Thermo Fisher Scientific). The reaction was incubated at 37 °C for 60 min in a thermocycler and the enzyme was removed immediately afterwards by an RNeasy MinElute Cleanup Kit (Qiagen) according to the manufacturer's instructions. DNase-treated and purified RNAs were used for subsequent analysis.

Quantification of 5-mC by LC-MS/MS. Quantification of 5-mC by LC-MS/MS was performed as previously reported³⁰, with the following modifications: 0.5 U rSAP (NEB) was used instead of alkaline phosphatase (Sigma-Aldrich). The mass transitions of *m/z* 258.0–126.1 (5-mC), *m/z* 274.0–142.1 (5-hmC), *m/z* 271.2–140.1 (5-fC), *m/z* 286.1–156.1 (5-caC) and *m/z* 244.1–112.0 (cytosine, C) were monitored and recorded, a series of concentrations of pure authentic nucleoside standards (C, from 50 nM to 2,000 nM, Sigma-Aldrich; 5-mC, from 0.5 nM to 50 nM, Sigma-Aldrich; 5-hmC, Santa Cruz, 5-fC and 5-caC, Berry & Associates, from 0.1 nM to 50 nM) were run for every batch of experiments to obtain their corresponding stand curves. Concentrations of nucleosides in mRNA samples were deduced by fitting the signal intensities into the stand curves. The ratios of 5-mC/G or 5-mC/U were subsequently calculated. Relative oxidation amounts were compared with 5-mC/U%, 0 min as 100%.

Dot blot. Dot blot assays for 5-mC, 5-hmC and 5-caC quantification in 90 °C denatured RNAs or DNAs were conducted as previously reported³. In brief, RNAs or DNAs were spotted onto a nylon membrane (GE Healthcare). The membrane was dried and crosslinked twice with 200,000 μ g cm⁻² ultraviolet light. The membrane was blocked in 5% BSA in PBS + 0.1% Tween-20 for 1 h before transfer into blocking solution supplemented with 5-mC or other modification antibody and incubated overnight at 4 °C. After secondary antibody incubation and wash, dot blots were visualized using SuperSignal West Femto Chemiluminescent Substrate (Thermo Fisher Scientific) by a chemiluminescent imaging system. The same amounts of denatured DNAs were degraded by TURBO DNase (Thermo Fisher Scientific) as negative control. To remove possible contaminating genomic DNAs, all RNAs samples were treated by the DNase.

Plasmid constructs. Full-length mouse *Socs3* or *Adar1* was PCR amplified using reverse transcribed RNAs from BMMCs. Tet2 eukaryotic expression vector was obtained as previously reported⁶. Mouse Tet2 mutant forms were as follows: Tet2_{HxD}, HS(H/Y)R(D/A)QQ; Tet2 Δ_{α -KG, T(R/M)I(S/F)LVLYRH, CTN(R/G)RCSQN; and Tet2 Δ_{DNA} , (W/R)SMYYNGC(K/E)FAR(S/N). They were generated by PCR-based amplification of the construct coding the wild-type protein and subcloned into the pCMV-Myc-N (Clontech). Wild-type *Adar1*, *Adar1*_{E861A} and *Adar1* Δ dsRNA³¹ (delete N456–G743) amplicons were subcloned into the pcDNA3.1-Flag-C (Invitrogen) vector. The *Socs3* and *Socs3*_{C-to-G} (chromosome 11: 117967529, 522, 518, 507, 485) full length were constructed into pcDNA3.1-HA-N (Thermo Fisher Scientific) vector. The 3' UTR of *Socs3* and the editing mutants *Socs3* Δ (chromosome 11: 117967036) was subcloned into pMIR-REPORT Luciferase (Thermo Fisher Scientific) vector. All constructs were confirmed by DNA sequencing.

eCLIP-seq. Biological replicates of BMMCs that had different culture start dates and crosslinked end dates were collected. eCLIP was conducted as previously reported¹¹, with the following modifications. Ultraviolet-crosslinked (first 400 mJ cm⁻² and then again at 200 mJ cm⁻²) BMMCs (4 \times 10⁷) were lysed in lysis buffer (50 mM Tris-HCl (pH 7.4), 100 mM NaCl, 1% NP-40, 0.1% SDS, 0.5% sodium deoxycholate and protease inhibitors) and sonicated. Lysates were treated with RNase I (Thermo Fisher Scientific) to fragment RNA and DNase I to remove DNA, while Tet2 antibody was bound to dynabeads in lysis buffer for 1 h at room temperature. Beads were washed three times using lysis buffer and incubated with proteins lysates for 4 h at 4 °C. A 3' RNA adaptor was ligated onto the RNA with T4 RNA ligase (NEB). Protein-RNA complexes were run on a 4–12% gradient Bis-Tris Gels (Invitrogen), transferred to PVDF membranes, and RNA was isolated off the membrane identically to standard eCLIP. A fraction of sample was used for western blot of CLIPed endogenous Tet2, indicating regions excised for eCLIP library preparation. After purification, RNAs were reverse transcribed with Superscript III reverse transcriptase (Invitrogen) with nested specific primer and a protected reverse PCR primer as previously reported³², free primer was removed (ExoSap-IT, Affymetrix) and a 3' DNA adaptor was ligated onto the cDNA product with T4 RNA ligase (NEB). Libraries were then amplified with Premix Taq PCR mix (Takara). Adapters and primers were designed according to the commercial indexing and sequencing

primers. Sequencing reads were processed and mapped according to eCLIP procedure. Peaks were identified using a 'valley seeking' algorithm, in which a peak is called if the valley of certain depth are found on both sides³³. Peaks were filtered with peak height above 5 as cut off. Enriched motifs in CLIP peaks were analysed by homer software using strand-specific sequences from peak regions as inputs.

RIP assay. RIP was conducted as previously reported³⁴. For endogenous RIP, cell lysates were made from wild-type or Tet2 knockout BMMCs in polysome lysis buffer (100 mM KCl, 5 mM MgCl₂, 10 mM HEPES pH 7.0, 0.5% NP40) supplemented with DTT, protease inhibitor cocktail (Roche) and RNase Inhibitor (Promega) on ice. Lysates were sonicated and stored at -80 °C. The Protein G magnetic beads were pre-blocked for 1 h with rotation in NT2 buffer supplemented with 5% BSA (50 mM Tris-HCl pH 7.4, 150 mM NaCl, 1 mM MgCl₂, 0.05% NP40). The antibody was then added for 4 h at 4 °C with rotation, followed by wash antibody-coated beads with 1 ml of ice-cold NT2 buffer four or five times. The cell lysate was thawed on ice and the insolubles were removed by centrifugation at 4 °C; 1% of total lysate was saved for input. Incubated cleared lysate and antibody were mixed for 2 h at 4 °C with rotation. Beads were washed four times with NT2 buffer and the RNA released by proteinase K for 30 min at 55 °C. Then RNA was isolated by adding TRIzol to the beads and glycogen (Thermo Fisher Scientific) added as a carrier to aid the precipitation reaction. For overexpression RIP experiments, the Myc-tagged Tet2 and its mutants, or haemagglutinin-tagged Socs3 or the mutant and Flag-tagged Adar1 were transfected into HEK293T cells or Tet2 knockout BMMCs for 36–48 h. Cells were collected in ice-cold polysome lysis buffer supplemented with protease inhibitor cocktail and RNase Inhibitor. For quantification in the RIP assay, cDNA amplicon signals were normalized by those from the reserved 1% input and used for comparison between experimental samples. When antibody against target was initially used in one type of cell, normalized signals in IgG groups were used for comparison with experimental samples. RNAs from both the reserved 1% input and the immunoprecipitated samples were treated with TURBO DNase, purified by TRIzol LS Reagent, and then reverse transcribed using random hexamers and ProtoScript II Reverse Transcriptase (NEB). PCR was used to amplify the target regions. The qPCR primers for the assay of the association of Adar1 with Socs3 3' UTR are in Extended Data Table 1.

RNA-mediated interference. BMMCs and HEK293T cells were transfected with siRNA (20 nM) through use of INTERFERin reagent (Polyplus Transfection). The mouse-specific siRNAs targeting Socs3 and Adar1 were designed and synthesized by GenePharma (Shanghai). Sequences of siRNAs were as follows: Socs3 siRNA 5'-GCCUCAAUACUUUUAUA-3'; Adar1 siRNA 5'-GCCUGCGAUAAAGCAUGAA-3'; Tet2 siRNA 5'-CCAUCA CAUUGCUUCUUU-3'.

J2 dsRNA pull-down. J2 antibody (1:50) was incubated with total nuclear extracts for 2 h at 4 °C (Lysis buffer: 50 mM HEPES pH7.5, 50 mM KCl, 5 mM MgCl₂, 1 mM DTT, 1 × complete protease inhibitors and RNase Inhibitor). Protein G-magnetic beads (Thermo Fisher Scientific) pre-blocked for 1 h with 1% BSA were added and incubated on a wheel for an additional 1.5 h at 4 °C. dsRNA-antibody complexes were eluted and dsRNAs were extracted using TRIzol LS Reagent (Invitrogen). RNA treatment and qPCR analysis were performed as in the RIP assay. The qPCR primers for validation of the Socs3 mRNA are in Extended Data Table 1.

meRNA-IP. The unmethylated control RNA and modified control RNA were obtained from *in vitro* transcription by using T7 RNA polymerase (Thermo Fisher Scientific). The total RNA of wild-type and Tet2 knockout BMMCs was extracted using TRIzol reagent and added with the 1% controls. RNA immunoprecipitation using anti-5-mC or other modifications was performed as previously reported without fragmentation³⁵. In brief, 10 µg total RNA was incubated for 2 h at 4 °C with 2 µg of affinity antibody in meRNA-IP buffer (150 mM NaCl, 0.1% NP-40, 10 mM Tris-HCl, pH 7.4). The mixture was then immunoprecipitated by incubation with Protein G beads (Thermo Fisher Scientific) at 4 °C for an additional 1 h. After extensive washing using meRNA-IP buffer, bound RNA was eluted from the beads with TRIzol reagent and ethanol precipitated. RNA treatment and qPCR analysis were performed as in the RIP assay. The qPCR primers of the unmethylated and modified controls are in Extended Data Table 1. The PCR primers for Socs3 mRNA were the same as in the J2 dsRNA pull-down assay. Signals in the qPCR assay were calculated as in the RIP assay.

Bisulfite-PCR sequencing. DNAs and RNAs isolated from BMMCs were bisulfite-converted using an EZ DNA Methylation-Lightning Kit or an EZ RNA Methylation Kit, with modifications described in bisulfite sequencing (Zymo) according to the manufacturer's instructions. The RNAs were treated as in the RIP assay. The treated RNA was reverse transcribed using random hexamers and ProtoScript II Reverse Transcriptase (NEB). PCR was used to amplify the target regions. The PCR primers are in Extended Data Table 1. The amplicons were subcloned, and ten clones were selected and sequenced to calculate the methylation rate of each cytosine.

RNA-seq analysis. RNA-seq analysis was performed as previously reported⁶. TopHat and Cufflinks were used for data analysis with mm10 as reference³⁶. FRKM

(total fragments/(mapped reads (M) × exon length (kilobases)) was calculated using cuffnorm for mRNA level quantification. HTSeq and DESeq were used for gene expression variation analysis (above twofold and $P < 0.05$, calculated by DESeq software on the basis of a negative binomial distribution)^{37,38}. Single-nucleotide mutation was analysed as previously reported^{39,40}. Filters were added for picking out mutations in mRNAs: (1) splice site information was added using a refGene.gtf file for excluding mutations there; (2) trimmed 10 nucleotides at both ends of sequencing reads, which could introduce biases; (3) with a quality score threshold of 25, a coverage threshold of 5 uniquely mapped reads; (4) a mutation supporting reads threshold of 2, and mutation rate between 0.1 and 0.95; (5) a mutation rate in DNA data under 0.05; (6) picking out group-specific mutants with mutation rates in one group three times higher than those in the other group.

RNA bisulfite high-throughput sequencing. Total RNAs were isolated by TRIzol reagent. Poly-A tailed RNAs were enriched by a GenElute mRNA Miniprep Kit (Sigma-Aldrich). The mRNAs were treated with TURBO DNase, purified by an RNeasy MinElute Cleanup Kit (Qiagen). Treated mRNAs with 0.5% unmethylated RNA controls from lambda genome were bisulfite-converted using an EZ RNA Methylation Kit, with some modifications (Zymo Research). In brief, 500 ng of mRNAs were converted using three cycles of 10-min denaturation at 70 °C followed by 45 min at 54 °C. RNA separation from bisulfite solution, desulfonation and purification were performed following the standard protocol of the kit. Strand-specific libraries were constructed following the 'TruSeq stranded mRNA sample preparation guide' from Illumina for 150PE sequencing using HiSeq3000. Clean data were processed as described in RNA-seq analysis. Read mapping and methylcytosine calling were analysed by BS-RNA⁴¹ using converted mm10 and lambda genomes as references. Splice site information was added using a refGene.gtf file during read mapping. Cytosines with a methylation rate above 0.1 and at least two reads supporting methylation in both technical and biological replicates of one group and below the non-conversion rate of each of the replicates of the other group (WT1 replicate 1: 0.0015; WT1 replicate 2: 0.0015; KO1 replicate 1: 0.0017; KO1 replicate 2: 0.0016; WT2 replicate 1: 0.0012; WT2 replicate 2: 0.0013; KO2 replicate 1: 0.0012; KO2 replicate 2: 0.0012) were chosen as group-specific cytosines.

In vitro RNA editing and Adar1 binding assays. The 3' UTRs of Socs3 mRNAs were obtained from *in vitro* transcription by using T7 RNA polymerase (Thermo Fisher Scientific). Adar1-Flag-overexpressed HEK293T whole-cell lysates (1 mg) were incubated for 2 h at 4 °C with anti-Flag beads (Sigma-Aldrich). Adar1-containing immunocomplexes were washed twice with cell lysis buffer and incubated with 500 ng RNA substrate and 300 µg nuclear extracts of BMMCs in 22 mM Tris-HCl (pH 7.5), 40 mM KCl, 10 mM NaCl, 6.5% glycerol, 0.5 mM DTT, 0.1 mM 2-mercaptoethanol, 0.05% NP-40 and RNase Inhibitor for 4 h at 30 °C. The RNA was recovered by TRIzol extraction and ethanol precipitation. For the Adar1 binding assay, the beads from incubation with RNA substrate and nuclear extracts of BMMC were washed three times with ice-cold NT2 buffer (50 mM Tris-HCl pH 7.4, 150 mM NaCl, 1 mM MgCl₂, 0.05% NP40). The beads were resuspended by TRIzol reagent. RNA was precipitated followed by reverse transcription and qPCR analysis.

5-mC affinity pull-down coupled with LC-MS/MS analysis. BMMCs (1 × 10⁸) were swollen for 20 min in 50 ml RSB buffer (10 mM Tris-HCl pH 8.0, 10 mM NaCl, 0.5% NP-40, 3 mM MgCl₂) and centrifuged at 2,000g for 5 min at 4 °C. The pellets consisting of nuclei were lysed by 90 min incubation in two volumes of nuclear lysis buffer (420 mM NaCl, 20 mM HEPES pH 7.9, 20% v/v glycerol, 2 mM MgCl₂, 0.2 mM EDTA, 0.1% NP40, protease inhibitor and 0.5 mM DTT). After centrifugation, protein concentrations in the extracts were measured by BCA assay and stored at -80 °C. Ten micrograms of 5'-biotinylated cytosine or 5-mC RNAs were immobilized on 75 µl of Dynabeads MyOne C1 (Invitrogen) by incubating for 1 h at room temperature in a total volume of 350 µl of binding buffer (1 M NaCl, 10 mM Tris-HCl pH 8, 1 mM EDTA pH 8, and 0.05% NP-40 and RNase Inhibitor). Beads containing immobilized RNAs were then incubated with 1 mg of nuclear extracts of BMMCs in a total volume of 600 µl of protein binding buffer (50 mM Tris-HCl pH8, 150 mM NaCl, 1 mM DTT, 0.25% NP-40 and complete protease inhibitors in the presence of RNase Inhibitor) for 2 h at 4 °C. Protein-complex-containing beads were washed extensively and eluted. LC-MS/MS analysis was conducted with the experimental workflows as previously reported⁶.

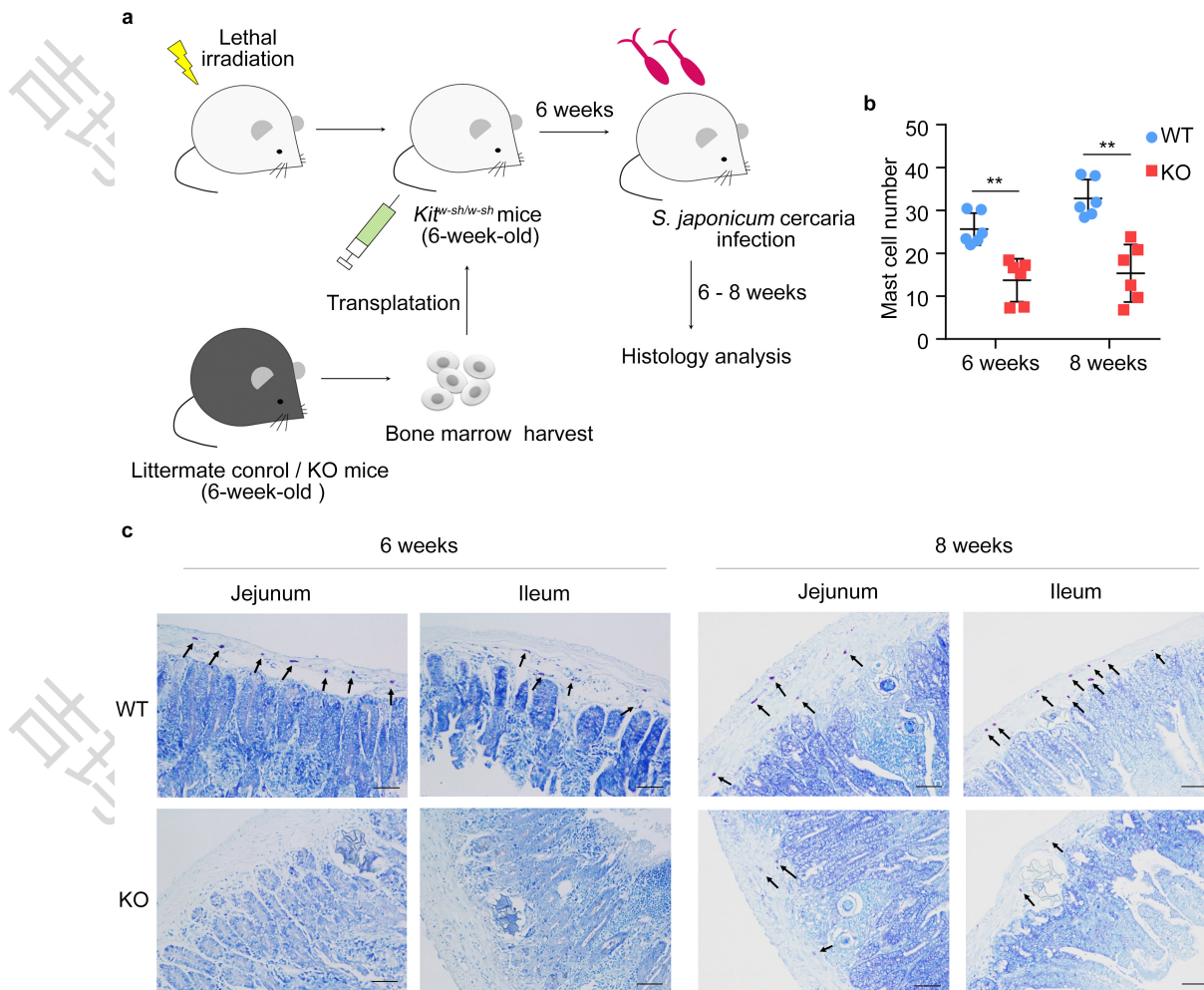
Assay of luciferase reporter gene expression. HEK293T cells were transfected with a mixture of the appropriate luciferase reporter plasmid, pRL-TK-renilla luciferase plasmid and the appropriate additional constructs using jetPEI (Polyplus). The total amount of plasmid DNA was equalized by empty control vector. Luciferase activity was measured with a Dual-Luciferase Reporter Assay System according to the manufacturer's (Promega) protocols after 24 h. Data were normalized for transfection efficiency by the division of firefly luciferase activity with that of renilla luciferase.

Statistical analysis. Error bars displayed throughout the paper represent s.e.m. or s.d. and were calculated from triplicate technical or triplicate biological

replicates described in figure legends. Sample sizes were chosen by standard methods to ensure adequate power, and no randomization of weight and sex or blinding was used for animal studies. Data shown are representative of three independent experiments, including histological images, blots and gels. No statistical method was used to predetermine sample size. Statistical significance was determined using unpaired two-sided Student's *t*-tests; **P* < 0.05; ***P* < 0.01.

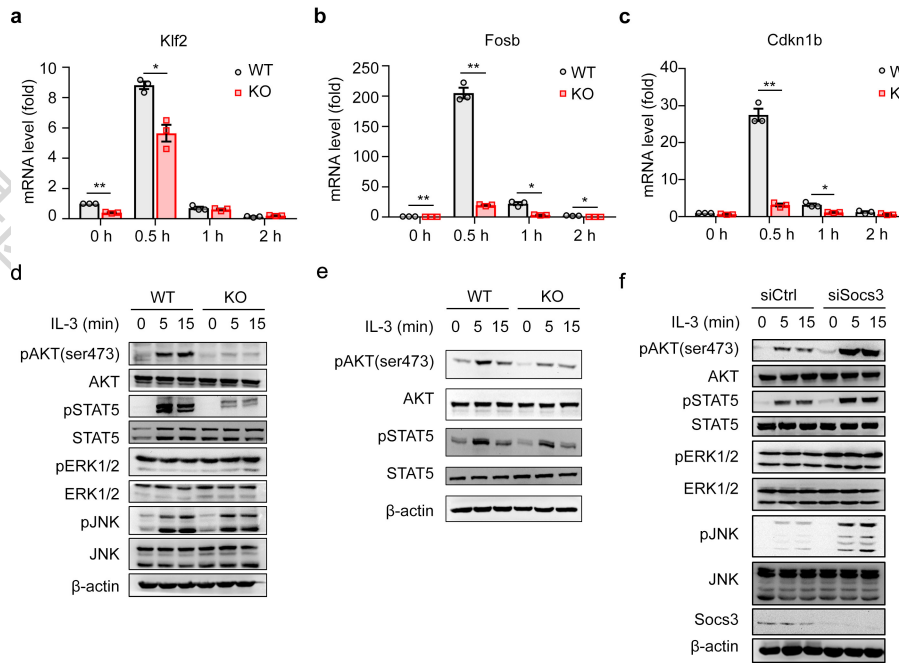
Data availability. The data that support the findings of this study are available from the corresponding author upon reasonable request. The RNA sequencing data have been deposited in NCBI Sequence Read Archive under accession numbers GSE100559, GSE100560 and GSE100719.

28. Rittirsch, D., Huber-Lang, M. S., Flierl, M. A. & Ward, P. A. Immunodesign of experimental sepsis by cecal ligation and puncture. *Nat. Protocols* **4**, 31–36 (2009).
29. Yu, M. *et al.* Tet-assisted bisulfite sequencing of 5-hydroxymethylcytosine. *Nat. Protocols* **7**, 2159–2170 (2012).
30. Li, X. *et al.* Transcriptome-wide mapping reveals reversible and dynamic N¹-methyladenosine methylome. *Nat. Chem. Biol.* **12**, 311–316 (2016).
31. Liddicoat, B. J. *et al.* RNA editing by ADAR1 prevents MDA5 sensing of endogenous dsRNA as nonself. *Science* **349**, 1115–1120 (2015).
32. Austin, E. G. *et al.* Improvements to the HITS-CLIP protocol eliminate widespread mispriming artifacts. *BMC Genomics* **17**, 338 (2016).
33. Zhang, C. & Darnell, R. B. Mapping *in vivo* protein–RNA interactions at single-nucleotide resolution from HITS-CLIP data. *Nat. Biotechnol.* **29**, 607–614 (2011).
34. Keene, J. D., Komisarow, J. M. & Friedersdorf, M. B. RIP-Chip: the isolation and identification of mRNAs, microRNAs and protein components of ribonucleoprotein complexes from cell extracts. *Nat. Protocols* **1**, 302–307 (2006).
35. Dominissini, D., Moshitch-Moshkovitz, S., Salmon-Divon, M., Amariglio, N. & Rechavi, G. Transcriptome-wide mapping of N⁶-methyladenosine by m⁶A-seq based on immunocapturing and massively parallel sequencing. *Nat. Protocols* **8**, 176–189 (2013).
36. Trapnell, C. *et al.* Differential gene and transcript expression analysis of RNA-seq experiments with TopHat and Cufflinks. *Nat. Protocols* **7**, 562–578 (2012).
37. Anders, S., Pyl, P. T. & Huber, W. HTSeq—a Python framework to work with high-throughput sequencing data. *Bioinformatics* **31**, 166–169 (2015).
38. Anders, S. & Huber, W. Differential expression analysis for sequence count data. *Genome Biol.* **11**, R106 (2010).
39. Ramaswami, G. *et al.* Identifying RNA editing sites using RNA sequencing data alone. *Nat. Methods* **10**, 128–132 (2013).
40. Peng, Z. *et al.* Comprehensive analysis of RNA-seq data reveals extensive RNA editing in a human transcriptome. *Nat. Biotechnol.* **30**, 253–260 (2012).
41. Liang, F. *et al.* BS-RNA: an efficient mapping and annotation tool for RNA bisulfite sequencing data. *Comput. Biol. Chem.* **65**, 173–177 (2016).



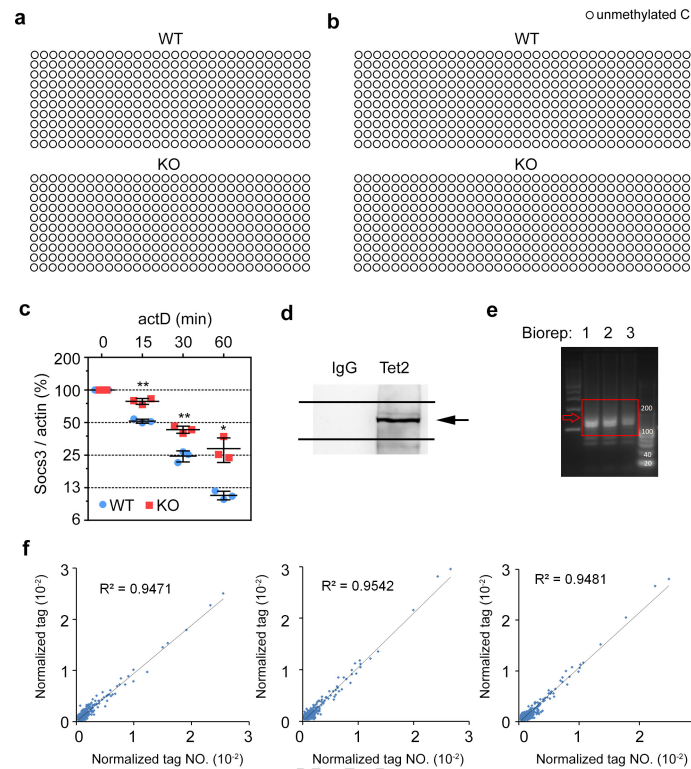
Extended Data Figure 1 | Tet2 promotes mast cell expansion during parasite infection. **a**, *In vivo* experimental design of transplantation and infection studies with bone marrow cells from Tet2-deficient (knockout) and littermate control (wild-type) mice. **b**, Quantitative assessment of toluidine blue-positive mast cells in the intestinal tissues ($n = 6$ biologically independent mice). **c**, Representative photomicrographs

of toluidine blue-stained tissue sections derived from *Kit^{W-sh/W-sh}* mice transplanted with bone marrow cells from the indicated genotypes. Arrows indicate mast cells. Scale bars, 50 μm . * $P < 0.05$, ** $P < 0.01$, unpaired two-sided Student's *t*-test. Mean and s.d. of n samples (**b**). Data are representative of three independent experiments with similar results (**c**).



Extended Data Figure 2 | Impaired IL-3 signalling pathway in Tet2-deficient myeloid cells. **a–c**, qPCR analysis of mRNA levels of indicated genes in wild-type (WT) and Tet2-deficient (KO) BMMCs treated with IL-3 (10 ng ml⁻¹). **d, e**, Immunoblot assays of the phosphorylated (p-) or total proteins in lysates of wild-type and knockout BMMCs (**d**) and bone marrow cells (**e**) stimulated with IL-3 for the indicated time. Bone marrow cells were collected from Tet2-deficient (knockout) and littermate control (wild-type) mice and pre-stimulated with IL-3 for 12 h.

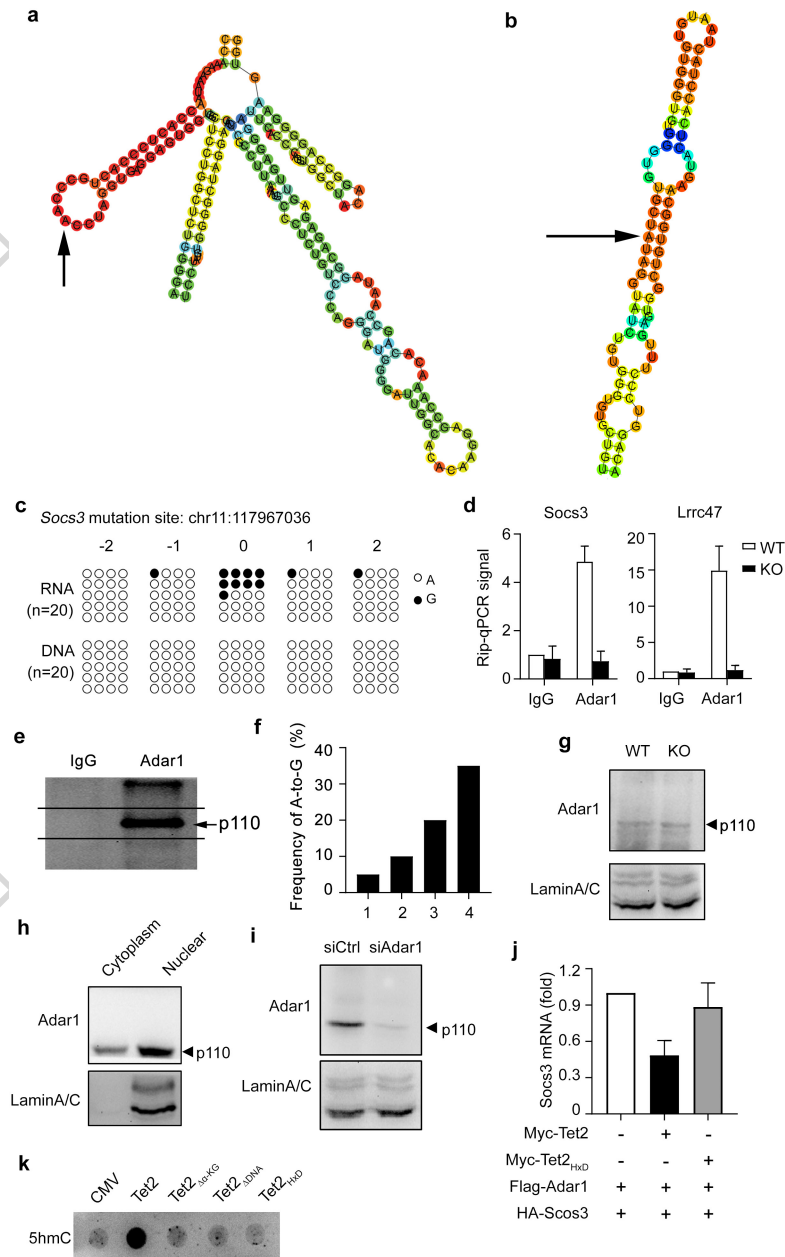
f, Immunoblot assays of the phosphorylated (p-) or total proteins in lysates of knockout BMMCs treated with non-targeting control siRNA (siCtrl) or Socs3-specific siRNA (siSocs3). Before being re-stimulated for the indicated times for subsequent analysis, BMMCs and bone marrow cells were starved for 12 h in the absence of cytokines. * $P < 0.05$, ** $P < 0.01$, unpaired two-sided Student's *t*-test. Mean and s.e.m. of triplicate biological replicates (**a–c**). Blots are representative of three independent experiments (**d–f**).



Extended Data Figure 3 | Tet2 binds and represses Socs3 mRNA.

a, b, Bisulfite-PCR assay of methylation states of CG dinucleotides in DNA regions of chromosome 11: 117969004-258 (**a**) or chromosome 11: 117969363-777 (**b**) in Tet2-deficient BMDCs and the control cells. **c**, Wild-type and knockout BMDCs were starved for 12 h in the absence of cytokines, and then treated with 5 mg ml⁻¹ actinomycin D (actD) for 0, 15, 30, 60 min. Socs3 mRNA decay was quantified by qPCR and normalization by β -actin. **d**, Immunoblot of Tet2 immunoprecipitation during CLIP. Black line indicates region excised for CLIP library preparation. **e**, PCR amplification products from CLIP experiments

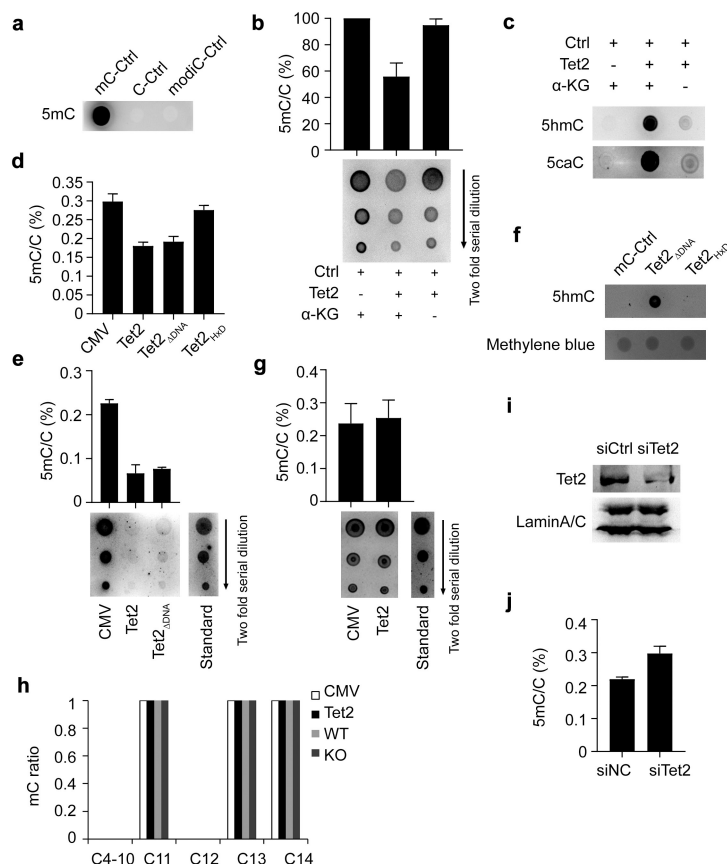
before indexing. Red box indicates gel region where DNA products were extracted for further indexing and high-throughput sequencing. Biorep 1, 2 and 3 are biological replicates from three BMDC samples which have different culture start dates and crosslinked end dates. **f**, Pairwise correlation analysis between biological replicates with normalized tag numbers in common peaks (from left to right: biorep 1 versus biorep 2, biorep 1 versus biorep 3, biorep 2 versus biorep 3). * $P < 0.05$, ** $P < 0.01$, unpaired two-sided Student's *t*-test. Mean and s.d. of triplicate biological replicates (**c**). Blots are representative of three independent experiments (**d**).



Extended Data Figure 4 | Adar1 binds and represses *Socs3* mRNA.

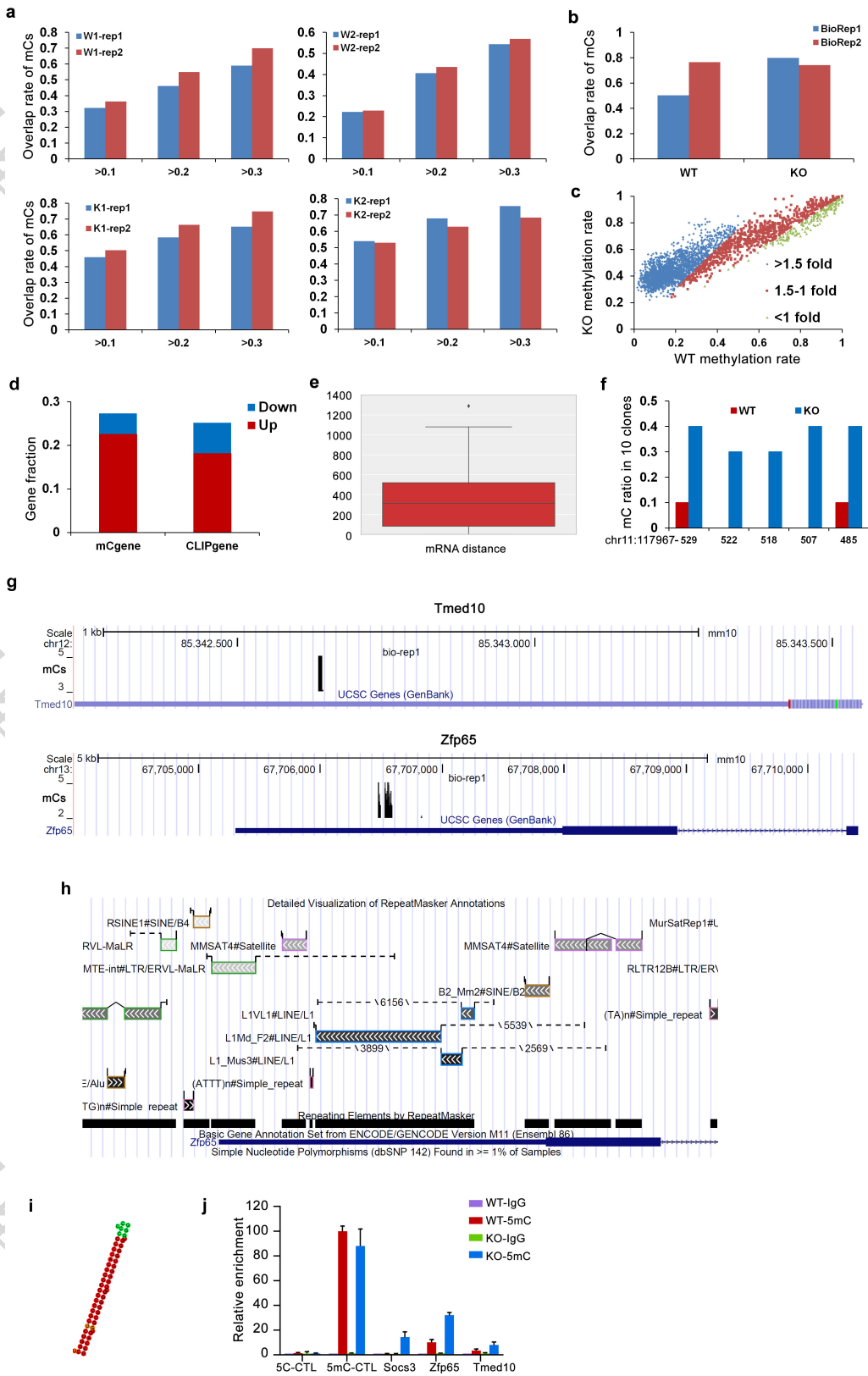
a, b, ViennaRNA prediction of secondary structure of sequences near editing sites in *Socs3* and *Lrrc47* 3' UTR. Arrows highlight edited adenosines. **c**, Experimental validation of the A-to-G mutation (0) and the nearby adenosines (-2, -1, 1, 2) in control BMMCs. **d**, RIP-qPCR analysis of *Socs3* or *Lrrc47* transcripts in RNAs from anti-Adar1 immunoprecipitated wild-type and knockout BMMCs lysates. **e**, Immunoblot of ADAR1 immunoprecipitation during CLIP. Black line indicates region excised for CLIP RNA preparation. **f**, RT-PCR sequencing assay of A-to-G mutation frequencies in *Socs3* mRNA from wild-type BMMCs at the indicated culture stages. **g**, Immunoblot of Adar1 protein

expression in BMMCs from wild-type and Tet2-deficient (knockout) mice. **h**, Immunoblot of Adar1 among cytoplasm and nuclear proteins of BMMCs. **i**, Immunoblot of Adar1 protein expression in BMMCs treated with non-targeting control siRNA (siCtrl) or Adar1-specific siRNA (siAdar1). **j**, qPCR analysis of HEK293T cells transiently transfected for 24 h with vectors coding haemagglutinin-tagged *Socs3*, Flag-tagged Adar1 and indicated Myc-tagged Tet2 mutants. **k**, Dot blot assays of 5-hmC levels in 10 ng DNA from Tet2- and Tet2 mutant-overexpressed HEK293T cells. Error bars, s.d. of triplicate technical replicates (**d, j**). Blots are representative of three independent experiments (**e, g-i, k**).



Extended Data Figure 5 | Tet2 promotes cytosine demethylation of mRNA. **a**, One microgram of *in vitro* transcribed RNAs containing 1% 5-mC, or 3% mixture of 5-hmC, 5-fC and 5-caC was analysed by dot blots using 5-mC antibody. **b**, **c**, The 5-mC levels in mRNAs (**b**) and 5-hmC and 5-caC levels of DNAs (**c**) from *in vitro* Tet2 oxidation assay with or without α-KG were analysed by dot blots. Twofold gradient dilutions of 20 ng synthetic *Socs3* mRNAs (**b**) and 10 ng DNAs (**c**) after oxidation were used for quantification. **d**, LC-MS for quantifying 5-mC levels of mRNAs from HEK293T cells overexpressing the indicated mutant forms of Tet2. **e**, **g**, Dot blot assays of 5-mC levels in 800 ng mRNAs (**e**) and 1 μg total RNA (**g**) from Tet2- and Tet2 $_{\Delta DNA}$ mutant-overexpressed HEK293T cells. Twofold gradient dilutions of 800 ng *in vitro* transcribed *Socs3*

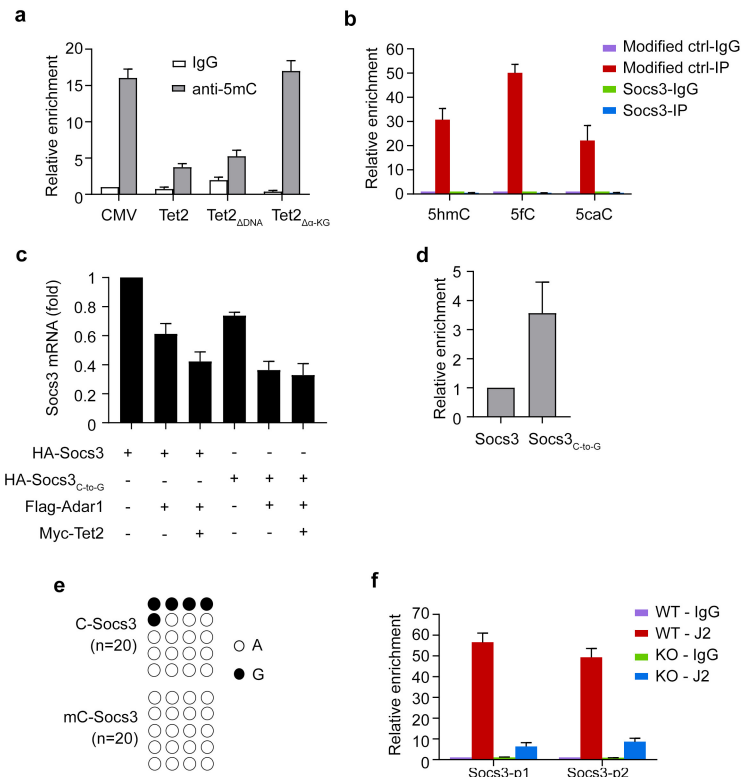
mRNAs containing 0.4% 5-mCs were used for the dilution curve of grey value-based quantification. **f**, *In vitro* RNA 5-mC oxidation assay of Tet2 mutants. The overexpressed Myc-tagged Tet2 mutants immunoprecipitated from HEK293T cells were subjected to *in vitro* oxidation. Oxidized RNAs pretreated with DNase were used for dot blot analysis of 5-hmC levels. **h**, Bisulfite-PCR assay of the 4th to 14th cytosines in tRNA^{Asp(GUC)} in Tet2-overexpressed HEK293T cells or Tet2-deficient BMMCs and the control cells. **i**, **j**, Immunoblot of Tet2 protein expression and LC-MS for quantifying 5-mC levels of mRNAs in HEK293T cells treated with non-targeting control siRNA (siCtrl) or Tet2-specific siRNA (siTet2). Mean and s.d of triplicate technical replicates (**b**, **d**, **e**, **g**, **j**). Blots are representative of three independent experiments (**a**-**c**, **e**-**g**, **i**).



Extended Data Figure 6 | See next page for caption.

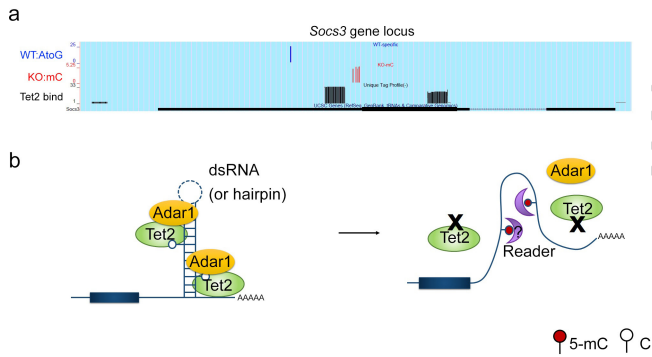
Extended Data Figure 6 | Specific profiles of mRNA 5-mCs in Tet2-deficient BMMCs. **a**, Overlap rates of methylcytosines with methylation levels above the indicated values in bisulfite sequencing assay between indicated technical replicates for Tet2-deficient (knockout, K1/2) and control (wild-type, W1/2) groups. **b**, Overlap rates of methylcytosines between the two biological replicates from common cytosines with read coverage above four. **c**, Methylcytosines in the knockout group were chosen, and mean methylation rates of these methylcytosine sites in both the wild-type and knockout groups were categorized with indicated variation folds and are presented in the scatter plot. Different colours indicate the variation of mean methylation levels of each of the methylcytosines in the knockout group compared with those in the wild-type group. **d**, Fraction of genes associated with knockout group-specific methylcytosines (mCgene) or CLIP peaks (CLIPgene) with variations of mRNA levels (>1.3-fold, up; <0.77-fold, down; $P < 0.05$) in the knockout group, compared with the control group. **e**, Exon-located CLIP peak and methylcytosine in the same gene were chosen, and the distance in mature mRNA between the CLIP peak boundary and the methylcytosine clusters

with the shortest gap was calculated. These distances for each of the genes are presented in the box plot (centre, median; box boundaries, 25% and 75% percentiles; whiskers, 1.5-fold interquartile range; diamond, outlier; $n = 11$ distance values). **f**, Bisulfite-PCR sequencing assay of cytosine sites with methylation-supported reads in the 3' UTR of *Sox3*. **g**, Genome browser views of gene loci containing 5-mCs in the Tet2-deficient group. Black signals indicate mean mC-supporting read numbers of all the replicates in the Tet2-deficient group. **h**, Genome browser view of the indicated region with RepeatMasker Viz containing the editing site in the 3' UTR of *Zfp65*. **i**, ViennaRNA prediction of secondary structure of sequences containing the methylation sites in the 3' UTR of *Tmed10*. **j**, qPCR analysis of gene transcripts from anti-5-mC immuno-selected RNAs from total RNAs of wild-type and knockout BMMCs. Unmethylated and methylated spike-ins as the negative and positive controls. Cytosine with coverage above 4, at least two reads supporting methylation and methylation level equal or above 0.1 was chosen as methylcytosine, considering both bioinformatic and biological significance. Mean and s.d of triplicate technical replicates (j).



Extended Data Figure 7 | Cytosine methylation in the 3' UTR of *Socs3* inhibits dsRNA structure. **a**, qPCR analysis of overexpressed *Socs3* transcripts from anti-5-mC immuno-selected RNAs from total RNAs of HEK293T cells transfected with Tet2 or Tet2 mutants. **b**, qPCR analysis of *Socs3* transcripts from specific-modification antibodies immuno-selected RNAs from total RNAs of wild-type BMDCs. Unmodified and modified spike-ins as the negative and positive controls. **c**, qPCR analysis of HEK293T cells transiently transfected for 24 h with vectors coding haemagglutinin-tagged wild-type *Socs3* or C-to-G mutant *Socs3*

(*Socs3*_{C-to-G}), with or without Flag-tagged Adar1 and Myc-tagged Tet2. **d**, RIP-qPCR analysis of *Socs3* 3' UTR levels in RNAs from Flag-tagged Adar1-immunoprecipitated HEK293T cell lysates overexpressed with *Socs3* or *Socs3*_{C-to-G} together with Adar1. Lysates (1%) were used for normalization as input. **e**, A-to-I editing rates in *Socs3* 3' UTR with cytosine or 5-mC after Adar1 editing *in vitro*. **f**, *Socs3* transcript levels determined by RT-qPCR from J2 immuno-selected dsRNA; p1, primer 1; p2, primer 2. Mean and s.d. of triplicate technical replicates (**a-d, f**). Data are representative of three independent experiments (**e**).



Extended Data Figure 8 | Schematic illustration of Tet2-mediated repression of *Socs3* via Adar1. **a**, Genome browser view of sequencing data on *Socs3* locus. Blue, A-to-G mutant reads in wild-type BMMCs; red, mean mC-supporting read numbers in knockout BMMCs; black, CLIP tag coverage. **b**, Tet2 promotes mRNA cytosine demethylation for effective formation of dsRNA which is bound by Adar1, leading to the suppression of *Socs3* expression at the post-transcriptional level.

Extended Data Table 1 | Sequences of PCR primers used in this study

Name	Prime	Sequence
<i>mSocs3_CLIP</i>	Forward	5' - GCGCTTTGATTTGGTTTGAT - 3'
	Reverse	5' - GGTTATTTCTTTGGCCAGCA - 3'
<i>mLrrc47_CLIP/RIP</i>	Forward	5' - CTGACAGGCTCCTGTAGGTGT - 3'
	Reverse	5' - TACAGCACACCCACAGATACCTAT - 3'
<i>mSocs3_RIP</i>	Forward	5' - CCTTTGACAAGCGGACTCTC - 3'
	Reverse	5' - GCCAGCATAAAAACCCTTCA - 3'
<i>mSocs3_P1</i>	Forward	5' - TATTCTGGGGGCGAGAAGAT - 3'
	Reverse	5' - ATCCAGGAACTCCCGAATG - 3'
<i>mSocs3_P2</i>	Forward	5' - ACATGGCACAAGCACAAAA - 3'
	Reverse	5' - GCTGGCACTTGAAAGAA - 3'
<i>mAdar1</i>	Forward	5' - TGAGCATAGCAAGTGGAGATACC - 3'
	Reverse	5' - GCCGCCCTTTGAGAACTCT - 3'
<i>unmodified-Ctrl</i>	Forward	5' - ATTGTATGTATTGGTTTATTG - 3'
	Reverse	5' - TTATCACATTCAAACATTAAT - 3'
<i>modified-Ctrl</i>	Forward	5' - TAGATAGTAAATATAATGTGAGA - 3'
	Reverse	5' - ATAAATCATCAACAAAACACAA - 3'
<i>mZfp65</i>	Forward	5' - GTGTGGAGACTTTGCCATT - 3'
	Reverse	5' - AAATGGTGTGACGTTTGGT - 3'
<i>mTmed10</i>	Forward	5' - CCAGGTAGAGTAGTCCATCCC - 3'
	Reverse	5' - AGGTTACTCTAGATGACCCA - 3'
<i>mKlf2</i>	Forward	5' - CTCAGCGAGCCTATCTTGCC - 3'
	Reverse	5' - CACGTTGTTTAGGTCCTCATCC - 3'
<i>mFosb</i>	Forward	5' - TTTTCCCGGAGACTACGACTC - 3'
	Reverse	5' - GTGATTGCGGTGACCGTTG - 3'
<i>mCdkn1b</i>	Forward	5' - TCAAACGTGAGAGTGTCTAACG - 3'
	Reverse	5' - CCGGGCCGAAGAGATTTCTG - 3'
<i>mβ-actin</i>	Forward	5' - AGTGTGACGTTGACATCCGT - 3'
	Reverse	5' - GCAGCTCAGTAACAGTCCGC - 3'
<i>mSocs3_editing</i>	Forward	5' - GACCTCTCTCCTCCAACGTG - 3'
	Reverse	5' - TGCAAAGTCTGAGTTGAACTGG - 3'
<i>mLrrc47_editing</i>	Forward	5' - CTGACAGGCTCCTGTAGGTGT - 3'
	Reverse	5' - GCATACCCACACCCAGATAC - 3'
<i>Socs3_bisulfite PCR</i>	Forward	5' - GTTTTAAGATTTTGTGTTTAAAAG - 3'
	Reverse	5' - AATACACCAACTTAAATACACAATC - 3'
<i>Socs3pro1_bisulfite PCR</i>	Forward	5' - AGAGTAGTGATTAATATTATAAGAAGAT - 3'
	Reverse	5' - TAAAATCTACAAAAAACTCCCC - 3'
<i>Socs3pro2_bisulfite PCR</i>	Forward	5' - TTTGGATTTGTTTATAGGTAATGT - 3'
	Reverse	5' - CTTAAAACATAAACCTCCAAAACCC - 3'

Life Sciences Reporting Summary

Nature Research wishes to improve the reproducibility of the work that we publish. This form is intended for publication with all accepted life science papers and provides structure for consistency and transparency in reporting. Every life science submission will use this form; some list items might not apply to an individual manuscript, but all fields must be completed for clarity.

For further information on the points included in this form, see [Reporting Life Sciences Research](#). For further information on Nature Research policies, including our [data availability policy](#), see [Authors & Referees](#) and the [Editorial Policy Checklist](#).

▶ Experimental design

1. Sample size

Describe how sample size was determined.

The sample size chosen for our animal experiments in this study was estimated based on our prior experience of performing similar sets of experiments.

2. Data exclusions

Describe any data exclusions.

No data were excluded.

3. Replication

Describe whether the experimental findings were reliably reproduced.

We at least independently repeated all the data once. All attempt to reproduce the results were successful

4. Randomization

Describe how samples/organisms/participants were allocated into experimental groups.

All animal- and cell-based samples in each of the group were included and no method of randomization was applied.

5. Blinding

Describe whether the investigators were blinded to group allocation during data collection and/or analysis.

Blinding is not relevant to our study, as we need to know the genotypes of the mouse strains.

Note: all studies involving animals and/or human research participants must disclose whether blinding and randomization were used.

6. Statistical parameters

For all figures and tables that use statistical methods, confirm that the following items are present in relevant figure legends (or in the Methods section if additional space is needed).

n/a Confirmed

- The exact sample size (n) for each experimental group/condition, given as a discrete number and unit of measurement (animals, litters, cultures, etc.)
- A description of how samples were collected, noting whether measurements were taken from distinct samples or whether the same sample was measured repeatedly
- A statement indicating how many times each experiment was replicated
- The statistical test(s) used and whether they are one- or two-sided (note: only common tests should be described solely by name; more complex techniques should be described in the Methods section)
- A description of any assumptions or corrections, such as an adjustment for multiple comparisons
- The test results (e.g. P values) given as exact values whenever possible and with confidence intervals noted
- A clear description of statistics including central tendency (e.g. median, mean) and variation (e.g. standard deviation, interquartile range)
- Clearly defined error bars

See the web collection on [statistics for biologists](#) for further resources and guidance.

► Software

Policy information about [availability of computer code](#)

7. Software

Describe the software used to analyze the data in this study.

RNA-seq: Tophat (2.1.0) & Cufflinks (2.2.1) & HTseq (0.6.1) & DEseq (1.20.0);
Bisulfite-seq: BS-RNA (1.0); CLIP: gscrypts (1.1) & STAR (2.4.0) & Homer (4.8)

For manuscripts utilizing custom algorithms or software that are central to the paper but not yet described in the published literature, software must be made available to editors and reviewers upon request. We strongly encourage code deposition in a community repository (e.g. GitHub). *Nature Methods* [guidance for providing algorithms and software for publication](#) provides further information on this topic.

► Materials and reagents

Policy information about [availability of materials](#)

8. Materials availability

Indicate whether there are restrictions on availability of unique materials or if these materials are only available for distribution by a for-profit company.

No restriction on availability of materials

9. Antibodies

Describe the antibodies used and how they were validated for use in the system under study (i.e. assay and species).

The detailed information on all antibodies were provided in the method section: Mice and reagents. Those antibodies are all commercially available, and have validation notes in the supplier's websites.

10. Eukaryotic cell lines

a. State the source of each eukaryotic cell line used.

HEK293T cells were obtain from ATCC.

b. Describe the method of cell line authentication used.

None of the cell lines have been authenticated.

c. Report whether the cell lines were tested for mycoplasma contamination.

The cell lines were not tested for mycoplasma contamination.

d. If any of the cell lines used are listed in the database of commonly misidentified cell lines maintained by [ICLAC](#), provide a scientific rationale for their use.

No commonly misidentified cell lines were used.

► Animals and human research participants

Policy information about [studies involving animals](#); when reporting animal research, follow the [ARRIVE guidelines](#)

11. Description of research animals

Provide details on animals and/or animal-derived materials used in the study.

Both male and female C57BL/6 mice of 6-8 weeks. The transgenic mouse lines: Tet2^{-/-}(C57BL/6), Kitw^{-sh/w-sh}(C57BL/6).

Policy information about [studies involving human research participants](#)

12. Description of human research participants

Describe the covariate-relevant population characteristics of the human research participants.

The research did not involve human research participants.